Effect of Clay Dispersion on the Synergism Between Clay and Intumescent Flame Retardants in Polystyrene

Yajun Chen,[1,2] Zhengping Fang,[1,2] Chunzhuang Yang,[1] Yu Wang,[1] Zhenghong Guo,[2] Yan Zhang[2]

[1]*Institute of Polymer Composites, Zhejiang University/Key Laboratory of Macromolecular Synthesis and Functionalization, Ministry of Education, Hangzhou 310027, China*
[2]*Laboratory of Polymer Materials and Engineering, Ningbo Institute of Technology, Zhejiang University, Ningbo 315100, People's Republic of China*

Received 18 February 2009; accepted 30 June 2009
DOI 10.1002/app.31068
Published online 10 September 2009 in Wiley InterScience (www.interscience.wiley.com).

ABSTRACT: Different formulations were designed to evaluate the effect of organically modified clay (DK4) on the combustion behavior of polystyrene (PS) containing an intumescent flame retardant, poly(4,4-diaminodiphenyl methane spirocyclic pentaerythritol bisphosphonate) (PDSPB). The results of transmission electron microscopy reveal that DK4 selectively dispersed in the PDSPB phase. An investigation of thermogravimetric analysis revealed that the thermal stability of PS resin showed no obvious change with the addition of PDSPB and DK4, but the residue increased. From the results of cone calorimetry, we observed that there were two steps during combustion. The dispersion of DK4 played an important role in improving the thermal stability and the flammability of the PS/PDSPB/DK4 nanocomposites. In the first step, DK4 was restricted in the PDSPB phase; there was no synergistic effect. A synergistic effect occurred in the second step when clay had a homogeneous distribution, in which the peak heat release rates were reduced by about 40 and 61% compared to the pure PS. A model of combustion behavior was developed according to these results. The synergistic mechanism was caused by the formation of the silicoaluminophosphate (SAPO) structure formed by reactions between PDSPB and DK4. Field emission scanning electron microscopy characterization showed that such an SAPO structure led to a ceramic-like residue after burning.
© 2009 Wiley Periodicals, Inc. J Appl Polym Sci 115: 777–783, 2010

Key words: clay; flame retardance; intumescence; polystyrene; thermal properties

INTRODUCTION

Polystyrene (PS) is used in many fields, such as automobiles, furniture, electronic casings, interior decor, and architectural materials. However, because of its chemical constitution, the polymer is easily flammable, has drippings, and emits much smoke during combustion, so flame retardancy becomes an important requirement for PS.

For more than a decade, potential environmental problems associated with organobromine flame-retardant systems have motivated the search for non-halogen-based approaches to reduce polymer flammability. Initially, researchers focused on the development of new phosphorus-based intumescent flame retardants (IFRs), and numerous publications and patents have been issued in this area.[1–4] Recently, a novel phosphorous nitrogen-containing IFR, poly(4,4-diaminodiphenyl methane spirocyclic pentaerythritol bisphosphonate) (PDSPB), was synthesized in our laboratory and has shown efficient flame retardancy for acrylonitrile-butadiene-styrene copolymer (ABS).[5]

At the same time, polymer–clay nanocomposites have attracted a great deal of interest. The unique characteristic of this new approach to flame-retardant polymeric materials is the dual benefit of reduced peak heat release rates (PHRRs) and improved physical properties, a combination not usually found with conventional flame retardants. A significant number of articles have been published on this topic, and some have shed light on the mechanism[6–9] by which clay nanocomposites have reduced flammability.

A derived approach has recently emerged that leads to the development of polymer flame-retardant layered silicate nanocomposites. In the past decade, an increasing number of studies have been reported on thermoset and thermoplastic polymers containing classical flame retardants and nanoparticles. Combinations of IFRs and organoclays have been studied, and a synergistic effect has been found. Bourbigot and coworkers[10,11] reported the performances of polyamide 6 nanocomposite as char-forming agents in intumescent formulations and as mechanical reinforcement agents. Tang et al.[12] studied the synergistic effect between ammonium polyphosphate (APP) and clay in polypropylene nanocomposites. The flammability behavior was significantly improved because of the formation of ceramic-like structures in

Correspondence to: Z. Fang (zpfang@zju.edu.cn).
Contract grant sponsor: National Natural Science Foundation of China; contract grant number: 50873092.

© 2009 Wiley Periodicals, Inc.

the intumescent char shield. In our laboratory, Ma et al.[13] observed the synergistic flame-retardation effect between clay and PDSPB in ABS nanocomposites. The synergism was caused by the formation of a silicoaluminophosphate (SAPO) structure formed by reactions between the phosphoric acid generated on heating from PDSPB and clay. Bourbigot et al.[10] reported that the nanodispersed clay allowed the thermal stabilization of a phosphorocarbonaceous structure in the intumescent char. Pack et al.[14] found that the clays aggregated into ribbonlike structures, and these ribbons might have partially explained the synergy due to the better distribution of the heat and improved the mechanical properties of the melt at high temperatures.

However, not all of the IFR and nanofillers have synergistic effects in all polymers. A recent article by Hussain et al.[15] showed that the addition of organoclay to an epoxy and phosphinate system resulted in PHRR and total released heat values that were higher than the system without the organoclay. Morgan[16] said the reason for this flame-retardancy antagonism was unclear, but the lack of uniform clay dispersion may have been responsible. So, it can be assumed that the dispersion of the nanoparticles in flame-retarded composites should be a key factor in obtaining significant synergies. The examination of the relationship between the dispersion of clay and the properties of the polymer flame-retarded layered silicate nanocomposites was the goal of this study.

In this study, an organically modified clay (DK4) and PDSPB were used to constitute a flame-retarded formulation for PS. The focus of this study was to investigate the effect of the dispersion of DK4 in the IFR PS resin.

EXPERIMENTAL

Materials

PS (666D) was obtained from Yanshan Petrochemical Co. (Beijing, China). The organically modified clay, coded as DK4, was supplied by Zhejiang Fenghong Clay Products (Anji County, Zhejiang Province, China), which was ion-exchanged with dioctadecyl dimethyl ammonium chloride. PDSPB was synthesized by condensation polymerization according to procedures published previously,[6] and its structure is shown here:

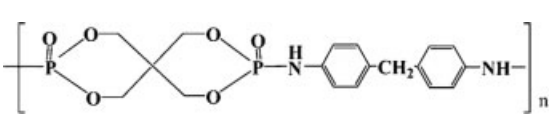

Preparation of the composites

The PS/DK4, PS/PDSPB, and PS/PDSPB/DK4 composites were prepared via melt compounding at 180°C in a Thermo Haake Rheomix (USA) with a screw speed of 60 rpm, and the mixing time was 8 min for each sample. The mixed samples were transferred to a mold and preheated at 180°C for 3 min, then pressed at 20 MPa, and successively cooled to room temperature while the pressure was maintained to obtain composite sheets for further measurement. The formulations prepared are shown in Table I.

TABLE I
Formulations of the Samples

Number	Sample code	Proportion (g)		
		PS	PDSPB	clay
1	PS	100	0	0
2	PS/clay-1	100	0	4
3	PS/clay-2	100	0	8
4	PS/PDSPB	80	20	0
5	PS/PDSPB/clay-1	80	20	4
6	PS/PDSPB/clay-2	80	20	8

Characterization

Transmission electron microscopy (TEM) was used to examine the dispersion of clay in the composites. TEM micrographs were obtained with a JEM-1200EX electron microscope (JEOL Corporation, Japan). The samples for TEM observation were ultrathin-sectioned with a microtome equipped with a diamond knife. The sections (200–300 nm in thickness) were cut from a piece about 1 $\times$1 mm^2, and they were collected in a trough filled with water and placed on 200-mesh copper grid.

Thermogravimetric analysis (TGA) was done in a TA SDTQ600 thermal analyzer (TA Instruments, USA) at a scanning rate of 10°C/min under air from 30 to 600°C.

The flammability of the samples was characterized by a cone colorimeter (Fire Testing Technology Limited, United Kingdom) according to ISO 5660 at an incident flux of 35 kW/m^2 with a cone-shaped heater. All sample plates, with dimensions of 10 cm $\times$10 cm $\times$1.5 mm, were placed in aluminum foil and then in a box with the same dimensions in the horizontal position. The cone data reported here are the averages of three replicated measurements.

Morphological studies of the char residue after cone colorimeter tests were performed with field emission scanning electron microscopy (FEI Sirion, The Netherlands).

Dynamic mechanical analysis was made with a TA Instruments Q800 dynamic mechanical analyzer at a frequency of 1 Hz from 30 to 150°C at a heating rate of 5°C/min. The single-cantilever bending mode was chosen.

RESULTS AND DISCUSSION

Clay nanoscale dispersion characterization

The nanoscale dispersion of the clay in the polymer was of utmost importance, as the type of dispersion

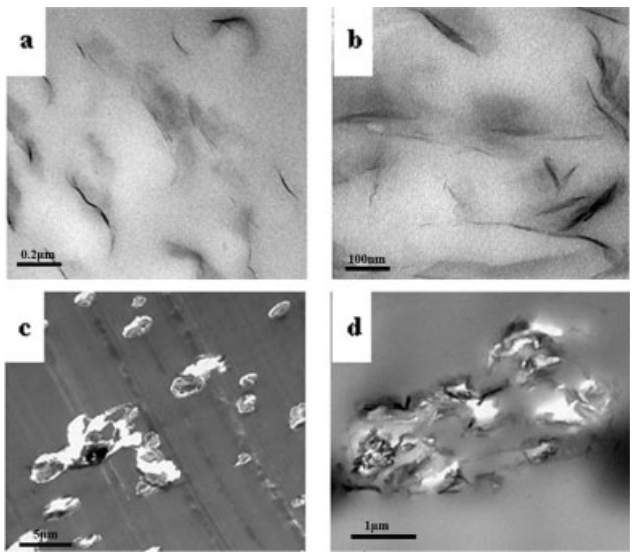

Figure 1 TEM photographs of (a,b) PS/4% DK4 and (c,d) PS/PDSPB/4% DK4 samples.

determined the mechanical and thermal properties of the nanocomposites.[17] The PS/DK4 and PS/PDSPB/DK4 nanocomposite samples, each containing a mass fraction of 4% of an organically treated clay, were analyzed by TEM (Fig. 1).

The TEM micrographs showed that the clay was well dispersed throughout the polymer in the PS/DK4 nanocomposites [Fig. 1(a)]. Individual clay layers along with two- and three-layer particles were observed to be well dispersed in the polymer matrix [Fig. 1(b)]. In addition, large intercalated tactoids (multilayer particles) were also visible. In the TEM photograph for the PS/PDSPB/DK4 nanocomposites [Fig. 1(c,d)], the gray continuous region corresponded to the PS phase, and the PDSPB appeared as deep gray islands (break during preparation). The black lines corresponded to clay layers, which were almost dispersed in the PDSPB phase. Moreover, in the interphase region [Fig. 1(d)], a high density of dispersed clay particles was observed. However, the layered clay could not be found in the PS matrix.

Clay dispersion depends on the polarity difference between the two phases.[18] For the PS/PDSPB/DK4 nanocomposites, PDSPB had a higher polarity than PS, and preferential intercalation behavior was observed. Such preferential melt intercalation behavior was also found in ABS/brominated epoxy resin–antimony oxide/clay nanocomposites.[19]

Thermal analysis results

Figure 2 shows the TGA and differential thermogravimetry (DTG) curves of the pure PS, PS/DK4, PS/PDSPB, and PS/PDSPB/DK4 samples. The detailed TGA and DTG data, for example, initial decomposition temperature (T_{onset}; designated as the onset point at 10 wt % weight loss), temperature of maximum weight-loss rate (T_{max}), and yield of char residue at 500°C for pure PS and its composites are summarized in Table II.

For these nanocomposite samples, T_{onset} in the TGA curves and T_{max} in the DTG curves of the PS/PDSPB/DK4 nanocomposites in air were lower than those of the PS/DK4 and PS/PDSPB nanocomposites, which indicated the thermal reduction effect of DK4 with PDSPB. The reason for this phenomenon may have been that in the PS/PDSPB/DK4 samples, PS and PDSPB were phase-separated, and clay preferentially dispersed in the PDSPB phase [Fig. 1(c,d)]. DK4, limited in the PDSPB phase, could not effectively restrain the evolution of flammable volatiles and the ingress of oxygen to the PS phase. At the same time, the layered structure of clay acted as a barrier and could thus limit the release of phosphoric acid and nonflammable gas produced by

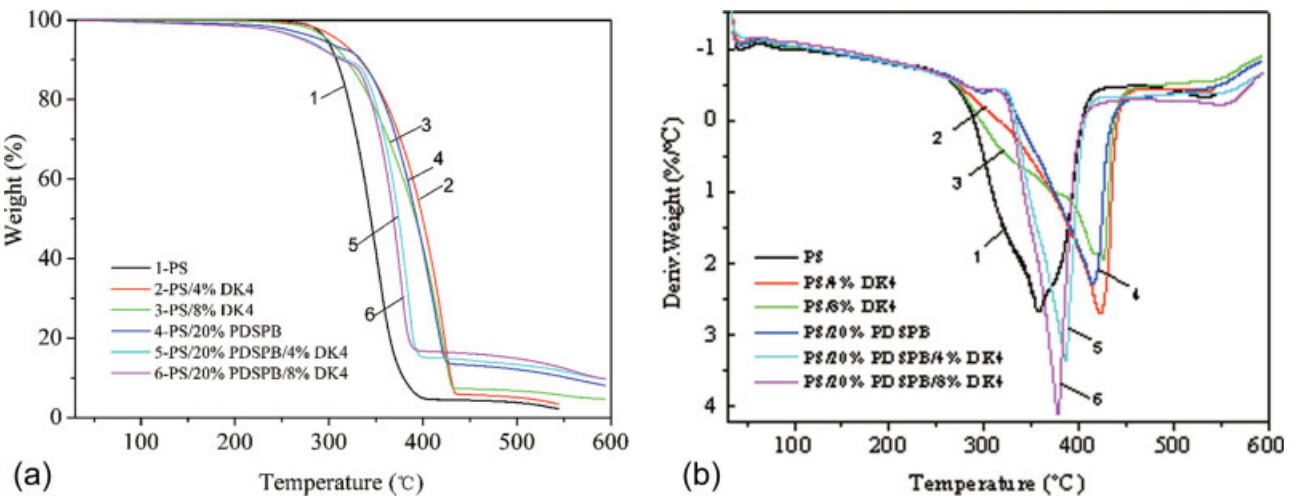

Figure 2 (a) TGA and (b) DTG curves of the pure PS, PS/DK4, PS/PDSPB, and PS/PDSPB/DK4 samples. [Color figure can be viewed in the online issue, which is available at www.interscience.wiley.com.]

TABLE II
Data of the TGA and DTG Thermograms of the Pure PS, PS/DK4 Nanocomposites, PS/PDSPB Blends, and PS/DK4/PDSPB Composites in Air at a Heating Rate of 10°C/min

Sample	T_{onset} (°C)	Char residue at 500°C (%)	T_{max} (°C)
PS	307.9	3.76	357.5
PS/clay-1	332.8	5.06	422.4
PS/clay-2	318.2	6.73	425.6
PS/PDSPB20	333.7	12.09	414.5
PS/PDSPB/clay-1	318.7	13.33	385.8
PS/PDSPB/clay-2	313.9	14.84	377.9

PDSPB. Therefore, both PDSPB and DK4 could not protect the polymer matrix from combustion.

The weight of the residue of PS/PDSPB/DK4 was greater than those of PS/DK4 or PS/PDSPB but was lower than the summation. This was explained by the fact that PDSPB reacted with DK4 to form an aluminophosphate structure and a ceramic-like structure in the 310–560°C temperature range during combustion,[10] which is shown later in Figure 7.

Flammability properties

Cone calorimetry is widely used to evaluate fire performance. It is one of the most effective bench-scale methods for studying the flammability properties of materials. Various parameters are obtained from cone measurements. The heat release rate (HRR), in particular, the PHRR, has been found to be the most important parameter in evaluating fire safety.

A comparison of the HRR data for pure PS and the PS/DK4, PS/PDSPB, and PS/PDSPB/DK4 nanocomposites is shown in Figure. 3. Table III shows the cone calorimetry data for the samples. The ignition time (t_{ign}) of the fire-retarded PS composites was lower than that of pure PS. The reason may have been that the introduction of clay (samples 2 and 3) or IFRs (sample 4) into PS decreased the apparent stability of the material and increased the ease of ignition. However, samples 5 and 6 had

TABLE III
Cone Calorimetry Data for the PS Samples at 35 kW/m^2

					5		6	
Sample	1	2	3	4	Step 1	Step 2	Step 1	Step 2
PHRR (kW/m^2)	736	579	505	502	527	446	488	284
Time to PHRR (s)	99	103	104	100	78	124	70	151
t_{ign} (s)	49	36	37	25	35		36	
THR (MJ/m^2)	50.8	49.4	49.3	47.2	47.9		48.2	

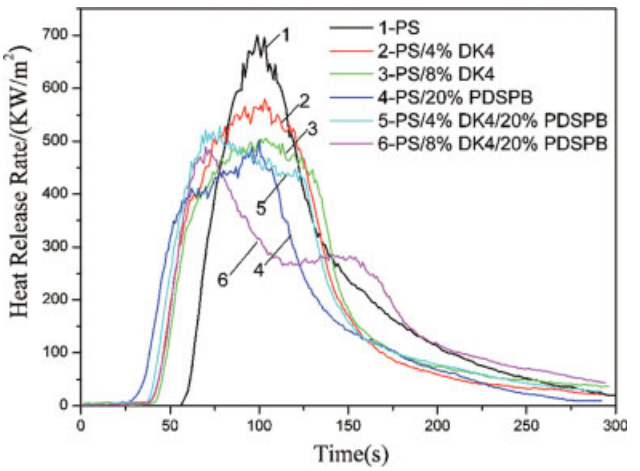

Figure 3 HRR of the PS, PS/DK4 nanocomposites, PS/PDSPB blends, and PS/PDSPB/DK4 composites. [Color figure can be viewed in the online issue, which is available at www.interscience.wiley.com.]

higher t_{ign} values than sample 4. The reason may have been due to the fact that the clay dispersed in the PDSPB phase delayed the early decomposition of PDSPB. Meanwhile, the total heat release (THR) of the PS/PDSPB/DK4 samples was lower than those of the pure PS and PS/DK4 samples, which illustrated that the combination of DK4 and PDSPB could make the fire-retarded material much safer in a fire. However, the THR of the PS/PDSPB/DK4 samples was a little higher than that of the PS/PDSPB samples because of the synergism occurring at later process during combustion, which is discussed later.

HRR, especially the PHRR, has been found to be one of the most important parameters in evaluating fire safety. The PHRR values of the PS/DK4 hybrids were reduced by about 21% (sample 2) and 30% (sample 3) in comparison with that of the pure PS. As for sample 4 (containing PDSPB), the PHRR was 31% lower than that of pure PS. The PHRR decreased still further when both PDSPB and DK4 were present (samples 5 and 6). The PHRR values of samples 5 and 6 were 28 and 35% lower, respectively, than that of pure PS. The value of PHRR decreased with increasing DK4 addition. For the composite where clay was preferentially dispersed in the domains, the introduction of clay reduced the domain size and enhanced the compatibility of composite. The domain size decreased with increasing clay addition.[18] According to this theory, in the PS/PDSPB/8% DK4 system, the PDSPB phase containing clay had a better dispersion compared to the PS/PDSPB/4% DK4 system, so the value of PHRR decreased.

As shown in Figure 3, it is interesting to note that the HRR curve of sample 6 showed two different steps. The first part (step 1) was from 0 to 110 s and contained the point of PHRR; the second part (step 2) was from 110 to 300 s and was shaped like a

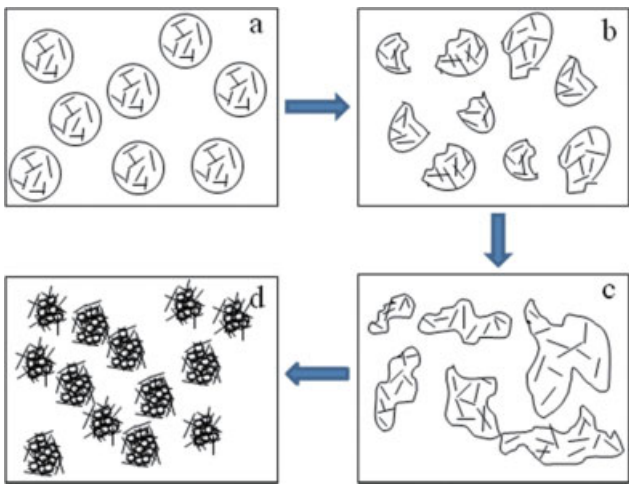

Figure 4 Schematic representation of the effect of DK4 and PDSPB on the improvement of the flame retardancy of the PS/PDSPB/DK4 nanocomposites. [Color figure can be viewed in the online issue, which is available at www.interscience.wiley.com.]

straight line. The same trend also existed for sample 5. The results from Table III show that the PHRR values in step 2 of sample 5 and sample 6 were reduced by about 40 and 61%, respectively, in comparison with the pure PS. Meanwhile, the t_{ign} of the PS/PDSPB/DK4 samples was higher than that of the PS/PDSPB samples. The effect of DK4 and PDSPB on the improvement of the flame retardancy of the PS/PDSPB/DK4 nanocomposites is illustrated by Figure 4.

In the PS/PDSPB/DK4 samples, PS and PDSPB were phase-separated, and most of the clay dispersed in the PDSPB phase [Fig. 4(a)]. At the beginning of combustion (0–110 s), the PDSPB phase deformed slightly, and the layered structure of clay acted as a barrier and thus limited the release of phosphoric acid and nonflammable gas produced by PDSPB. At the same time, DK4 restricted in the PDSPB phase could not effectively restrain the evolution of flammable volatiles and the ingress of oxygen to the PS phase [Fig. 4(b)]. Therefore, neither PDSPB nor DK4 could protect the polymer matrix from combustion. This was proven by the results of T_{onset} and T_{max}. With the extension of combustion time (110–300 s), the PDSPB melted into fluid, which made the DK4 dispersed in PDSPB tend to cover the surface of the nanocomposites [Fig. 4(c)]. Thus, the barrier character of the layered clay was efficiently improved. On the other hand, PDSPB further decomposed and released a lot of phosphoric acid and nonflammable gas. A synergistic effect occurred between IFR PDSPB and DK4. So the PHRR of step 2 decreased significantly, and the flame retardancy of the PS/PDSPB/DK4 nanocomposites was significantly improved.

The synergistic mechanism was caused by the formation of an SAPO structure formed by reactions between the phosphoric acid generated on heating from PDSPB and DK4. SAPO is a promising solid acidic catalyst and may have further favored the dehydration process and increased the char yield.[20] The formation of efficient char during the combustion process can act as a protective barrier in addition to the intumescent shield and can limit the oxygen diffusion to the substrate and/or inhibit the migration of liquid or gaseous decomposition products into the hot zone. This barrier may hinder the

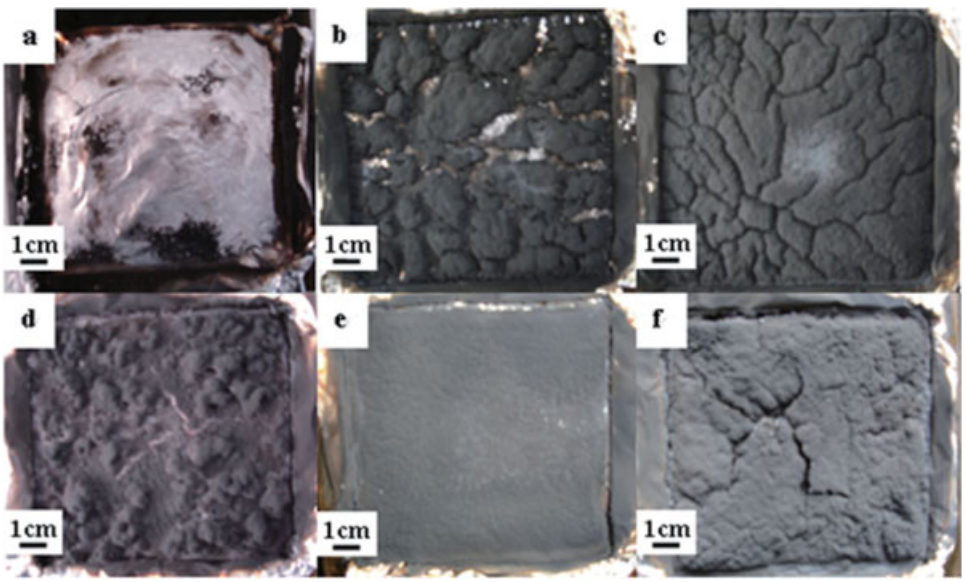

Figure 5 Digital photos of the residues for the (a) pure PS, (b) PS/4% DK4, (c) PS/8% DK4, (d) PS/PDSPB, (e) PS/PDSPB/4% DK4, and (f) PS/PDSPB/8% DK4 samples. [Color figure can be viewed in the online issue, which is available at www.interscience.wiley.com.]

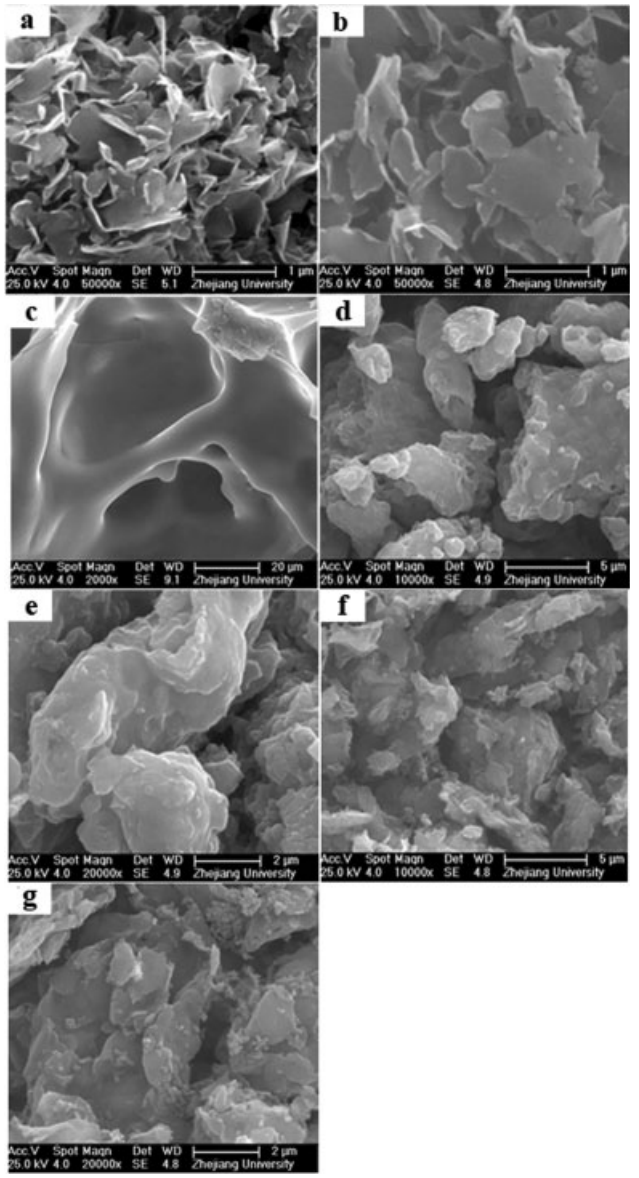

Figure 6 SEM micrographs of the residues for the (a) PS/4% DK4, (b) PS/8% DK4, (c) PS/PDSPB, (d,e) PS/PDSPB/4% DK4, and (f,g) PS/PDSPB/8% DK4 samples.

formation of cracks as well.[21] This is another reason for the improvement of flame retardancy in step 2. At higher temperatures, the phosphorocarbonaceous structure is degraded because of the collapse of the SAPO species. An amorphous ceramic-like alumina[10] containing orthophosphoric and polyphosphoric acid species is then created [Fig. 4(d)].

Figure 5 displays digital photos of the residues for the pure PS, PS/DK4, PS/PDSPB, and PS/PDSPB/DK4 samples after the cone calorimeter tests. The results show that the pure resin was almost burnt out and left negligible char [Fig. 5(a)]. The chars of the PS/DK4 nanocomposites were not integrated and had many surface cracks, although the char was thick when the concentration of DK4 was 8 wt % [Fig. 5(b,c)]. For the PS/PDSPB sample, an intact but thin swollen char layer with some small holes in it was formed [Fig. 5(d)]. However, both of the PS samples that contained DK4 and PDSPB showed extensive residue, and as the mass fraction of DK4 was increased from 4 to 8%, the quality of the residue improved; fewer cracks and a more continuous structure are observed [Fig. 5(e,f)].

Figure 6 shows the micromorphologies of chars from different samples. The residue of the PS/DK4 nanocomposites[22,23] had an intercalated structure and produced a little black carbonaceous char. A lot of the residual DK4 remained after combustion in air [Fig. 6(a,b)]. The char of the PS/PDSPB[5] composite exhibited a cohesive and dense structure. Some cavities could be seen on the char's surface. These cavities were pathways of gas fragments generated from the combustion and heat evolved during burning process [Fig. 6(c)]. Figure 6(d–g) shows the chars of the PS/PDSPB samples containing 4 and 8 wt % DK4, respectively, which were agglomeratic structures produced by the reaction of PDSPB and DK4. The residue of PS/PDSPB/DK4 showed a more tight and dense char layer compared to the PS/DK4 and PS/PDSPB systems. This indicated that the physical process of layer reassembling acted as a protective barrier in addition to the intumescent shield and could have limited the oxygen diffusion to the substrate or given a less disturbing low volatilization rate. A strong affinity between carbonaceous entities and clay mineral layers was seen, and this may have been the morphology of the ceramic-like structure. The sizes of agglomeration decreased with increasing DK4 addition. This was because in the PS/PDSPB/8% DK4 system, the PDSPB phase, containing clay, had a better dispersion compared to the

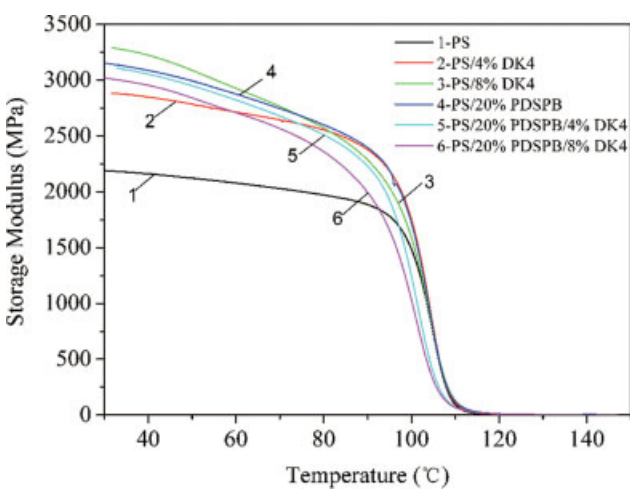

Figure 7 E' of the (1) PS, (2,3) PS/DK4 nanocomposite, (4) PS/PDSPB blend, and (5,6) PS/PDSPB/DK4 composite samples. [Color figure can be viewed in the online issue, which is available at www.interscience.wiley.com.]

PS/PDSPB/4% DK4 system, to which we referred earlier. The result is consistent with the schematic representation of Figure 4(d).

Dynamic mechanical analysis

The storage modulus (E') data of the PS, PS/DK4, PS/PDSPB, and PS/PDSPB/DK4 nanocomposites are shown in Figure 7.

Below 90°C, the E' values of these PS blends appeared to be much higher than that of the pure resin. For the PS/DK4 samples, E' improved with increasing DK4 addition. However, it decreased with increasing DK4 loading in the PS/PDSPB/DK4 system. The reason may have been the effects of clay on the compatibilization of PS and PDSPB. For the composite where clay was preferentially dispersed in the domains, the introduction of clay reduced the domain size and enhanced the compatibility of the composite. The domain size decreased with increasing clay addition.[18] The PS/PDSPB/8% DK4 system had a lower E' because of smaller PDSPB phases in the system. This was consistent with the results of PHRR in step 1.

CONCLUSIONS

A melt-blending method was used to prepare PS/DK4, PS/PDSPB, and PS/PDSPB/DK4 samples. An investigation of the thermal degradation behavior revealed that the thermal stability of the PS resin showed no obvious change with the addition of PDSPB and DK4, but the residue increased. From the results of cone calorimetry, we observed that there were two steps during combustion. A synergistic effect occurred in step 2, in which the PHRR values were reduced by about 40 and 61% in comparison with the pure PS. The dispersion of DK4 played an important role in improving the thermal stability and flammability for the PS/PDSPB/DK4 nanocomposites. If the DK4 was restricted in the PDSPB phase, there was no synergistic effect. A synergistic effect occurred when the clay had a homogeneous distribution. The synergistic mechanism was caused by the formation of an SAPO structure formed by reactions between the phosphoric acid generated on heating from PDSPB and DK4. SAPO is a promising solid acidic catalyst and may have further favored the dehydration process and increased the char yield. The morphology of a ceramic-like structure was clearly seen in the field emission scanning electron microscopy images.

References

1. Price, D.; Pyrah, K.; Hull, T. R.; Milnes, G. J.; Wooley, W. D.; Ebdon, J. R.; Hunt, B. J.; Konkel, C. S. Polym Int 2000, 49, 1164.
2. Chao, C. Y. H.; Wang, J. H. J Fire Sci 2001, 19, 137.
3. Zaikov, G. E.; Lomakin, S. M. J Appl Polym Sci 2002, 86, 2449.
4. Wei, P.; Li, H. X.; Jiang, P. K.; Yu, H. Y. J Fire Sci 2004, 22, 367.
5. Ma, H. Y.; Tong, L. F.; Xu, Z. B.; Fang, Z. P.; Jin, Y. M.; Lu, F. Z. Polym Degrad Stab 2007, 92, 720.
6. Beyer, G. J Fire Sci 2005, 23, 75.
7. Jang, B. N.; Wilkie, C. A. Polymer 2005, 46, 3264.
8. Bourbigot, S.; Bras, M.; Duquesne, Le, S.; Rochery, M. Macromol Mater Eng 2004, 289, 499.
9. Costache, M. C.; Jiang, D. D.; Wilkie, C. A. Polymer 2005, 46, 6947.
10. Bourbigot, S.; Bras, M. L.; Dabrowski, F.; Gilman, J. W.; Kashiwagi, T. Fire Mater 2000, 24, 201.
11. Dabrowski, F.; Bras, M. L.; Cartier, L.; Bourbigot, S. J Fire Sci 2001, 19, 219.
12. Tang, Y.; Hu, Y.; Wang, S. F.; Gui, Z.; Chen, Z. Y.; Fan, W. C. Polym Int 2003, 52, 1396.
13. Ma, H. Y.; Tong, L. F.; Xu, Z. B.; Fang, Z. P. Appl Clay Sci 2008, 42, 238.
14. Pack, S.; Si, M.; Koo, J.; Sokolov, J. C.; Koga, T.; Kashiwagi, T.; Rafailovich, M. H. Polym Degrad Stab 2009, 94, 306.
15. Hussain, M.; Varley, R. J.; Mathys, Z.; Cheng, Y. B.; Simon, G. P. J Appl Polym Sci 2004, 91, 1233.
16. Morgan, A. B. Polym Adv Technol 2006, 17, 206.
17. Morgan, A. B.; Harris, J. D.; Kashiwagi, T.; Chyall, L. J.; Gilman, J. W. Fire Mater 2002, 26, 247.
18. Chow, W. S.; Mohd Ishak, Z. A.; Karger-Kocsis, J. J Polym Sci Part B: Polym Phys 2005, 43, 1198.
19. Ma, H. Y.; Fang, Z. P.; Tong, L. F. Polym Degrad Stab 2006, 91, 1972.
20. Zanetti, M.; Camino, G.; Reichert, P.; Mulhaupt, R. Macromol Rapid Commun 2001, 22, 176.
21. Lv, P.; Wang, Z. Z.; Hu, K. L.; Fan, W. C. Polym Degrad Stab 2005, 90, 523.
22. Wang, J. Q.; Du, J. X.; Zhu, J.; Wilkie, C. A. Polym Degrad Stab 2002, 77, 249.
23. Hao, J. W.; Lewin, M.; Wilkie, C. A.; Wang, J. Q. Polym Degrad Stab 2006, 91, 2482.